Transition Metal Complexes with Sulfur Ligands. XXVIII*. Ruthenium Complexes of the Pentadentate Thioether Thiolate Ligands dpttd^{2-} (2,3,11,12-dibenzo-1,4,7,10,13-pentathiatridecane(−2)) and the Sterically Demanding Derivative $^{t}bu_4$-dpttd^{2-} (14,16,18,20-tetra(t-butyl)-2,3,11,12-dibenzo-1,4,7,10,13-pentathiatridecane(−2))**

DIETER SELLMANN†, GERHARD BINKER, MATTHIAS MOLL

Institut für Anorganische Chemie der Universität, D-8520 Erlangen, Egerlandstr. 1, F.R.G.

and CHARLES E. CAMPANA

Nicolet Corporation, P.O. 4370, Madison, Wis., U.S.A.

(Received November 17, 1986)

Abstract

The template alkylation of $Li_2[Ru(CO)_2(S_2C_6H_4)_2]$ ($S_2C_6H_4^{2-}$ = 1,2-benzenedithiolate(−2)) by $S(C_2H_4Br)_2$ yields $[Ru(CO)_2(dpttd)]$ (dpttd^{2-} = 2,3,11,12-dibenzo-1,4,7,10,13-pentathiatridecane-(−2)) which is thermally converted into the monocarbonyl complex [Ru(CO)(dpttd)]. The reactions of dpttd-H_2 or dpttd^{2-} with $[RuCl_2(PPh_3)_3]$, $[RuCl_2(DMSO)_4]$, $[RuCl_3(PhSCH_3)_3]$ and $RuCl_3(NO)\cdot xH_2O$ lead to [Ru(L)(dpttd)] and [Ru(L)(dpttd)]Cl (L = PPh_3, DMSO, $PhSCH_3$, NO), respectively, which are practically insoluble in all common solvents. Better soluble complexes are obtained with the new sterically demanding ligand $^{t}bu_4$-dpttd^{2-} = 14,16,18,20-tetra(t-butyl)-2,3,11,12-dibenzo-1,4,7,10,13-pentathiatridecane(−2); it is obtained in isomerically pure form by the reaction of tetrabutylammonium-3,5-di(t-butyl)-1,2-benzenethiolthiolate, $NBu_4[^{t}bu_2\text{-}C_6H_2S(SH)]$, with $S(C_2H_4Br)_2$ and yields on reaction with $[RuCl_2(PPh_3)_3]$ the very soluble $[Ru(PPh_3)_2(^{t}bu_4\text{-dpttd})]$ as well as $[Ru(PPh_3)(^{t}bu_4\text{-dpttd})]$. The ^1H NMR and ^{31}P NMR spectra indicate that in solution $[Ru(PPh_3)_2(^{t}bu_4\text{-dpttd})]$ exists as a mixture of diastereomers, whereas $[Ru(PPh_3)(^{t}bu_4\text{-dpttd})]$ forms one pair of enantiomers only. This was confirmed by an X-ray structure determination of a single crystal. $[Ru(PPh_3)(^{t}bu_4\text{-dpttd})]$ crystallizes in space group $P2_1/n$ with a = 10.496(4), b = 14.888(6), c = 32.382(12) Å, β = 98.04(3)°, Z = 4 and $D_{calc.}$ = 1.27 g/cm^3, R = 4.84; R_w = 5.06%; the ruthenium center is coordinated pseudooctahedrally by one phosphorus, two thiolate and three thioether S atoms.

Introduction

Sulfur coordination by sulfido, thiolato as well as thioether ligands plays an important role for the metal centers of many metal redox enzymes as for example in ferredoxines or nitrogenase [2]. In order to study the chemical properties of metal sulfur centers we have been investigating the coordination chemistry of transition metals with ethanedithiolate, *o*-benzenedithiolate as well as multidentate thioether thiolate ligands derived thereof [3]. The latter ones form complexes which are kinetically inert with respect to a complete metal sulfur ligand dissociation, in contrast to $[Fe(CO)_2(S_2C_6H_4)_2]^{2-}$ for example, which reacts with PMe_3 under loss of one $C_6H_4S_2^{2-}$ ligand yielding $[Fe(CO)_2(PMe_3)(S_2C_6H_4)]$ [4]. Often thiolato ligands form insoluble complexes, because bridging via thiolate S atoms leads to bi- or polynuclear species. This might be true also for a number of complexes with the multidentate ligand dpttd^{2-} (2,3,11,12-dibenzo-1,4,7,10,13-pentathiatridecane(2−)), whose synthesis as well as iron complexes we described recently [5]. Investigating the ruthenium chemistry of dpttd^{2-} we obtained preferentially insoluble complexes; therefore we synthesized also the sterically demanding tetra-t-butyl derivative $^{t}bu_4$-dpttd-H_2 = (14,16,18,20-tetra(t-butyl)-2,3,11,12-dibenzo-1,4,7,10,13-pentathiatridecane), whose ruthenium PPh_3 complexes are reported.

*For Part XXVII, see ref. 1.

**According to IUPAC rules this ligand might be named: 1,5-bis(2-mercapto-3,5-di-tert-butyl-phenylthio)-3-thiapentane; in concurrence with the unsubstituted dpttd-H_2, which has been introduced already, we prefer the name given in the title.

†Author to whom correspondence should be addressed.

0020-1693/87/$3.50

Experimental

General

All reactions were carried out in absolute solvents under nitrogen using the Schlenk tube technique. Starting materials were prepared according to literature methods: *o*-benzenedithiol [6], bis(β-bromethyl)sulfide [7], dpttd-H_2 [5], 3,5-di(t-butyl)-benzene-1,2-dithiol [8], $[RuCl_2(CO)_3(THF)]$ [9a], $Li_2[Ru(CO)_2(S_2C_6H_4)_2]$ [9b], $[RuCl_2(PPh_3)_3]$ [10], $[RuCl_3(PhSCH_3)_3]$ [11], $RuCl_3(NO)\cdot xH_2O$ [12] and $[RuCl_2(DMSO)_4]$ [13]. Spectra were run on Zeiss IR spectrometer IMR 16, Jeol FT-NMR spectrometer JNM-GX 270, Jeol NMR spectrometer JNM PMX 60 and Varian MAT 212 mass spectrometer.

Syntheses

[Ru(CO)(dpttd)]

To a solution of 850 mg (6 mmol) of *o*-benzenedithiol in 10 ml of THF are added at −78 °C 12 mmol of n-butyllithium (7.35 ml of a 1.6 M solution of n-butyllithium in n-hexane. After warming up to +20 °C the solution is added dropwise under stirring to 984 mg (3 mmol) of $[RuCl_2(CO)_3(THF)]$ in 60 ml of THF. The resulting solution turns orange and evolves CO. After 1 h of stirring, 740 mg (3 mmol) of bis(β-bromethyl) sulfide in 15 ml of THF are added. The solution is stirred for another 13 h, and its volume reduced *in vacuo* to *ca.* 30 ml. After addition of 35 ml of toluene the mixture is refluxed for 5 h. Upon cooling to 20 °C orange crystals precipitate which are filtered off and washed twice with 5 ml of THF/toluene (1:2) and 5 ml of methanol. Drying *in vacuo* for 1 day gives a yellow–orange powder. Yield: 410 mg (27%). *Anal.* Calc. for $C_{17}H_{16}ORuS_5$ (497.7): C, 41.03; H, 3.24. Found: C, 41.14; H, 3.05%.

[Ru(PPh$_3$)$_2$(dpttd)]

To a suspension of 2.52 g (2.6 mmol) of $[RuCl_2(PPh_3)_2]$ in 60 ml of THF is added a solution of 970 mg (2.6 mmol) of dpttd-H_2 in 25 ml of THF at 20 °C. After stirring for 30 min 600 ml of n-hexane are added and a green solid precipitates from the clear greenish solution. Yield: 1.42 g (54%). *Anal.* Calc. for $C_{52}H_{46}P_2RuS_5$ (994.3): C, 62.80; H, 4.66. Found: C, 64.58; H, 4.69%.

[Ru(PPh$_3$)(dpttd)]

A suspension of 497 mg (0.5 mmol) of $[Ru(PPh_3)_2(dpttd)]$ in 40 ml of THF is refluxed for 1.5 h. After cooling to 20 °C the turbid green colored solution is filtered and reduced to *ca.* 15 ml *in vacuo*. Addition of 400 ml of n-hexane precipitates a dark green solid which was filtered off, washed twice with 5 ml of n-hexane and dried *in vacuo*. Yield: 157 mg (43%). *Anal.* Calc. for $C_{34}H_{31}PRuS_5$ (732.2): C, 55.80; H, 4.30. Found: C, 54.34; H, 4.62%.

[Ru(DMSO)(dpttd)]

To a suspension of 185 mg (0.5 mmol) of dpttd-H_2 in 40 ml of methanol is added a solution of 54 mg (1 mmol) of $NaOCH_3$ in 10 ml of methanol. The resulting solution is added dropwise to an orange–yellow solution of 242 mg (0.5 mmol) of $[RuCl_2(DMSO)_4]$ in 50 ml of methanol and stirred for 30 min. The light brown solid which forms is filtered off and washed with 3 × 20 ml of methanol. Yield: 153 mg (56%). *Anal.* Calc. for $C_{18}H_{22}ORuS_6$ (547.8): C, 39.46; H, 4.05. Found: C, 42.56; H, 4.08%.

[Ru(PhSCH$_3$)(dpttd)]Cl

To a solution of 185 mg (0.5 mmol) of dpttd-H_2 in 40 ml of THF is added at −78 °C 1 mmol of n-butyllithium (0.6 ml of a 1.6 M solution of n-butyllithium in n-hexane). After warming up to 20 °C a solution of 290 mg (0.5 mmol) of $[RuCl_3(PhSCH_3)_3]$ in 30 ml of THF is added. Stirring for 15 min gives a green precipitate which is filtered off and washed with 2 × 5 ml of methanol. Yield: 115 mg (43%). *Anal.* Calc. for $C_{23}H_{22}ClRuS_6$ (543.8): C, 45.59; H, 3.99. Found: C, 40.91; H, 3.71%.

[Ru(NO)(dpttd)]Cl

To a dark red solution of 292 mg (~1 mmol) of $RuCl_3NO\cdot xH_2O$ in 30 ml of THF is added a solution of 370 mg (1 mmol) of dpttd-H_2 in 10 ml of THF. Within 4 days at 20 °C brown crystals precipitate; they are separated, washed with 2 × 5 ml of THF and dried *in vacuo*. Yield: 298 mg (56%). *Anal.* Calc. for $C_{16}H_{16}ClNORuS_5$ (534.8): C, 35.93; H, 3.02; N, 2.62. Found: C, 36.91; H, 3.47; N, 1.96%.

^{t}bu$_4$-dpttd-H$_2$

A solution of 2 g (7.9 mmol) of 3,5-di(t-butyl)-benzene-1,2-dithiol in 12 ml of THF and 7.9 mmol of NBu_4OH (7.9 ml of a 1 m solution of NBu_4OH in methanol) is heated to reflux, 0.98 g (4 mmol) of bis-(β-bromethyl)sulfide in 12 ml of THF are rapidly added and the resulting yellow–red solution is refluxed for another 20 min. After evaporation to dryness the residue is treated with 50 ml of n-hexane yielding a suspension which is filtered over Na_2SO_4 and silica 60. The filtrate is evaporated to dryness and the remaining oil is recrystallized from ether/methanol (20 °C/−30 °C) giving colourless crystals. Yield: 2.0 g (86%). *Anal.* Calc. for $C_{32}H_{50}S_5$ (595.1): C, 64.65; H, 8.42: Found: C, 64.69; H, 8.45%. Melting point (m.p.) 62–64 °C.

[Ru(PPh$_3$)$_2$(^{t}bu$_4$-dpttd)] and [Ru(PPh$_3$)(^{t}bu$_4$-dpttd)]

To a solution of 871 mg (0.91 mmol) of $[RuCl_2(PPh_3)_3]$ in 40 ml of THF is added a solution of 540 mg (0.91 mmol) of ^{t}bu$_4$-dpttd-H_2 in 10 ml of THF at 20 °C. The resulting green solution is stirred for 24 h. After reducing the volume of the solution to *ca.* 10

ml *in vacuo*, addition of 20 ml of methanol and storing at −30 °C, a microcrystalline light brown powder precipitates which was filtered and washed with 2×5 ml of methanol. Yield: 521 mg (47%). *Anal.* Calc. for $[Ru(PPh_3)_2(^tbu_4\text{-dpttd})] = C_{68}H_{78}P_2RuS_5$ (1218.6); C, 67.02; H, 6.45. Found: C, 67.01; H, 6.51%.

When the filtrates are slowly evaporated at 20 °C orange crystals of $[Ru(PPh_3)(^tbu_4\text{-dpttd})]$ separate out. They are filtered off and washed twice with 5 ml of methanol. Yield: 87 mg (10%). *Anal.* Calc. for $C_{50}H_{63}PRuS_5$ (956.4): C, 62.79; H, 6.64. Found: C, 62.75; H, 6.60%.

Crystal Growth and X-ray Structure Analysis of $[Ru(PPh_3)(^tbu_4\text{-dpttd})] = C_{50}H_{63}PRuS_5$

A single crystal with the approximate dimensions 0.60 mm×0.40 mm×0.20 mm was obtained from a THF/methanol mixture by slow evaporation of the solvents at 20 °C; it was sealed in a glass capillary without drying and mounted on a Nicolet R3 mE diffractometer, which was used for the determination of the unit cell dimensions and the data collection, respectively. Data were collected using the ω-scan ($3.5° < 2\theta < 45.0°$, $3.91 \leqslant \omega \leqslant 29.30°$/min). The relevant diffraction data are listed in Table I. The structure was solved by direct methods using the programs Nicolet EXTL and SHELXTL 5.1 [14].

TABLE I. Diffraction Data of $[Ru(PPh_3)(^tbu_4\text{-dpttd})]$

Space group	$P2_1/n$
Lattice constants	
a (Å)	10.496(4)
b (Å)	14.888(6)
c (Å)	32.382(12)
β (°)	98.04(3)
V (Å^3)	5010(3)
Z (M = 956.4)	4
$D_{calc.}$ (g/cm^3)	1.27
μ(Mo Kα) (cm^{-1})	5.7
λ(Mo Kα-graphite monochromator) (Å)	0.71073
Temperature (K)	296
Measured independent reflections	6562
with $F \geqslant 6\sigma(F)$	5124
R, R_w	4.84, 5.06

Results and Discussion

The ligand dpttd-H_2 is obtained by the template and hydrolysis reactions, respectively, according to eqn. (1) [5].

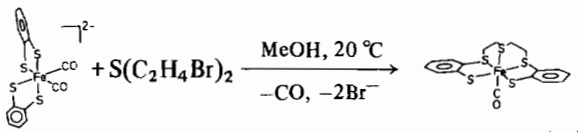

(1a)

$$[Fe(CO)(dpttd)] \xrightarrow[\text{reflux, } \sim 2.5 \text{ h}]{\text{HCl, THF}} \text{dpttd-}H_2 + CO + FeCl_2 \quad (1b)$$

The lability and cleavage of the Fe–CO bonds in $[Fe(CO)_2(S_2C_6H_4)_2]^{2-}$ obviously facilitate the formation of five membered $[FeS_2C_2]$ chelate rings resulting in high yields of [Fe(CO)(dpttd)].

If the same type of reaction is carried out with the analogous ruthenium complex $[Ru(CO)_2(S_2C_6H_4)_2]^{2-}$ according to eqn. (2) the first step of alkylation takes

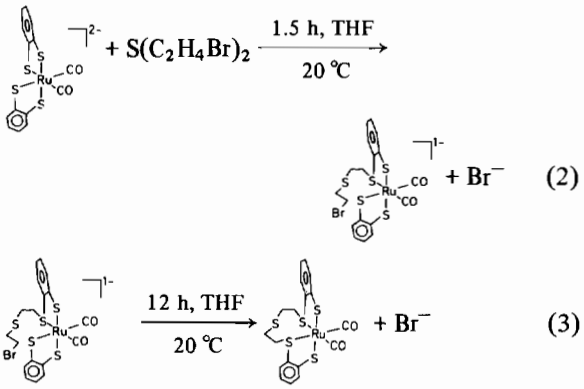

place fairly rapidly, but the second step needs considerably more time (eqn. (3)) than in the case of iron; the resulting compound is not a mono but a dicarbonyl complex. With ruthenium no metal CO bonds are cleaved generating free sites of coordination and consequently the ligand dpttd^{2-} can act as tetradentate ligand only; the reaction sequence shows the usually much higher kinetic stability of ruthenium *versus* iron complexes. Monitoring the reaction by IR spectroscopy (Fig. 1) it is seen that

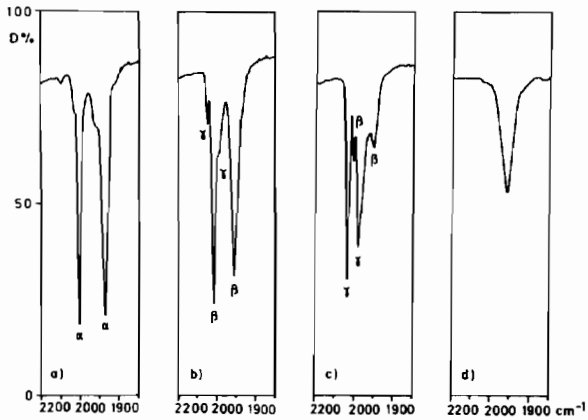

Fig. 1. IR monitoring of reaction (2) and (3) (ν(CO) region). (a) $[Ru(CO)_2(S_2C_6H_4)_2]^{2-} \triangleq \alpha$; (b) 1.5 h after addition of $S(C_2H_4Br)_2$ at 20 °C ($[Ru(CO)_2(S_2C_6H_4)(C_6H_4S_2C_2H_4SC_2H_4Br)] \triangleq \beta$; $[Ru(CO)_2(dpttd)] \triangleq \gamma$); (c) ~30 days after addition of $S(C_2H_4Br)_2$; (d) [Ru(CO)dpttd] in DMF (obtained according to eqn. (4).

the solution contains a mixture of the neutral $[Ru(CO)_2(dpttd)]$ and the monoalkylated monoanion of eqn. (2) even after 30 days at ambient temperatures.

Since we were rather interested in the mono carbonyl complex we refluxed the reaction mixture resulting from eqn. (3) for 5 h in a THF/toluene solution according to eqn. (4).

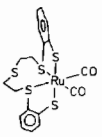

$$\xrightarrow[5\text{ h, reflux}]{\text{THF/toluene}} [Ru(CO)(dpttd)] + CO \quad (4)$$

After cooling the reaction solution to ambient temperatures orange crystals of [Ru(CO)(dpttd)] precipitated. [Ru(CO)dpttd] shows the characteristic absorptions of the $dpttd^{2-}$ ligand and a strong $\nu(CO)$ band at 1960 cm^{-1} in the KBr IR spectrum. In the ^1H NMR spectrum (d_7-DMF) the multiplets at 7.80–6.60 ppm and 4.00–3.05 ppm are assigned to the aromatic protons and C_2H_4-bridge protons, respectively, and the FD mass spectrum shows the molecular ion at $m/e = 498$. [Ru(CO)(dpttd)] is soluble only in DMF and DMSO. The CO ligand proved to be inert towards substitution under thermal conditions; UV irradiation of [Ru(CO)(dpttd)] led to decomposition.

It proved difficult to obtain further fully characterizable [Ru(L)(dpttd)] complexes. In these experiments we reacted for example $[RuCl_2(PPh_3)_3]$, $[RuCl_2(DMSO)_4]$, $[RuCl_3(PhSCH_3)_3]$ and $RuCl_3(NO)\cdot xH_2O$ with $dpttd^{2-}$ to get the corresponding [Ru(L)(dpttd)] and [Ru(L)(dpttd)]Cl, respectively, with L = PPh_3, DMSO, $PhSCH_3$ and NO. The isolated products contained undoubtedly the ligand $dpttd^{2-}$, as well as the different ligands L bound to ruthenium, as shown for example by IR spectroscopy; they were, however, so poorly soluble even in DMSO and DMF, that it was impossible to recrystallize them in order to get analytically pure compounds. The basic reason for this different behaviour with respect to the iron complexes may be the kinetic inertness of the ruthenium complexes, which eventually leads to completely different structures and favours the formation of insoluble polynuclear species by Ru–S(thiolate)–Ru bridging. Therefore we tried to synthesize the corresponding ligand from 3,5-di(t-butyl)benzene-1,2-dithiol, $^t bu_2$-$C_6H_2(SH)_2$ [8] anticipating that the

t-butyl groups would provide a steric protection of free sites of coordination at the ruthenium centers preventing the formation of Ru–S(thiolate)–Ru bridges.

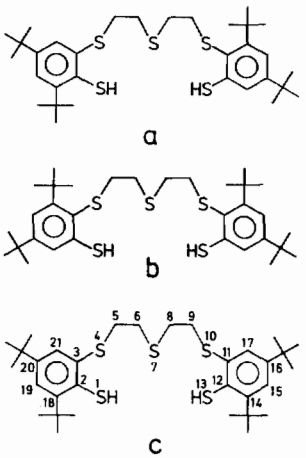

Fig. 2. Isomers of $^t bu_4$-dpttd-H_2.

In connecting two molecules of $^t bu_2$-$C_6H_2(SH)_2$ by alkylation with $S(C_2H_4Br)_2$ in order to generate the pentadentate $^t bu_4$-dpttd-H_2, three isomers are to be expected (Fig. 2).

Isomer c in which both of the remaining SH functions are sterically hindered was of special interest. Its complexes should show the most effective hindrance of metal thiolate metal bridging. Initial attempts to synthesize this isomer by a template synthesis analogous the synthesis of dpttd-H_2 failed. The reaction according to eqn. (5) yielded only a mixture

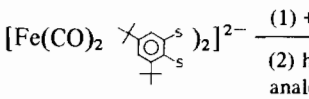

$$[Fe(CO)_2(\quad)_2]^{2-} \xrightarrow[\text{(2) hydrolysis analogous to eqn. (1)}]{\text{(1)} + S(C_2H_4Br)_2}$$

mixture of isomers a, b, and c (5)

of all isomers a–c which could not be separated; the templation of the thiolate groups by Fe^{2+} appeared rather to level the different character (with respect to steric environment as well as for example acidity) of the S atoms. We therefore tried to react free $^t bu_2$-$C_6H_2(SH)_2$ with $S(C_2H_4Br)_2$ in the presence of half an equivalent of NaOMe or LiOMe, but obtained again practically the same mixture of isomers. Since it could not be excluded, that even the 'hard' Na^+ or Li^+ ions exerted template effects *versus* the 'soft' thiolate groups we employed finally NBu_4OH as base in order to eliminate any undesired template effects expecting that in this case the sterically less hindered thiolate group would react faster than the hindered one. With NBu_4OH indeed isomer c formed in yields above 85% according to eqn. (6).

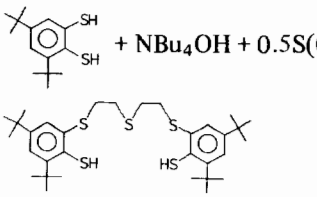

$$+ NBu_4OH + 0.5S(C_2H_4Br)_2 \xrightarrow[20\text{ min, reflux}]{\text{THF/methanol}}$$

$$+ NBu_4Br + H_2O \quad (6)$$

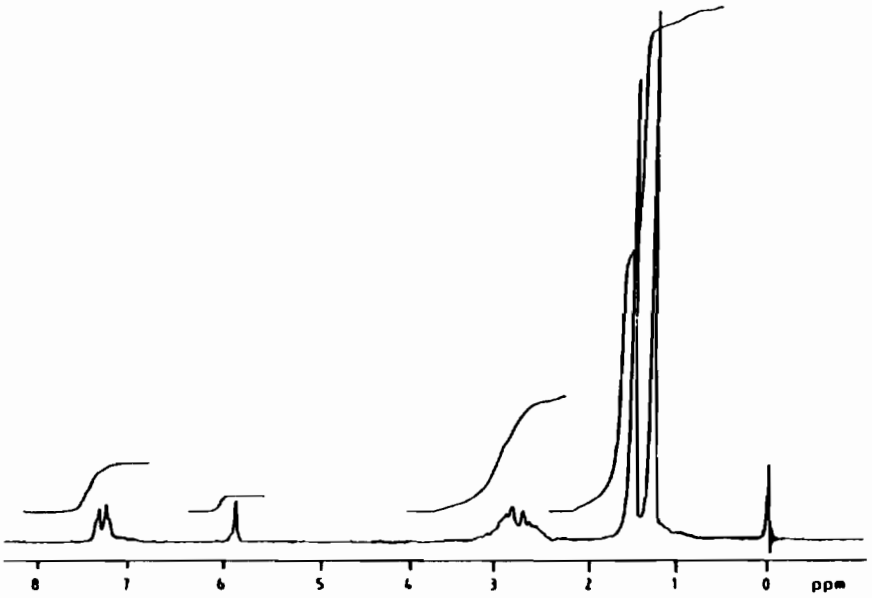

Fig. 3. ^{1}H NMR spectrum of ^{t}bu$_4$-dpttd-H$_2$ (in CCl_4).

After recrystallization ^{t}bu$_4$-dpttd-H$_2$ was obtained as colourless crystals and characterized by elemental analysis as well as spectroscopic means (see Table IV below). Particularly characteristic is the t-butyl region of the ^{1}H NMR spectrum (Fig. 3). It shows two sharp singlets of the four t-butyl groups at 1.50 and 1.30 ppm, respectively, in addition to the phenyl protons in the region of 7.35 to 7.10 ppm, the singlet of the two SH protons at 5.80 ppm and the multiplet of the C_2H_4 protons between 3.10 and 2.30 ppm. That the alkylation has taken place at the sterically less hindered thiol groups is inferred from the chemical shift of the SH protons of ^{t}bu$_4$-dpttd-H$_2$; they are low field shifted with respect to dpttd-H$_2$, probably due to the 'van der Waals' effect between SH and *ortho*-t-butyl groups [15].

In order to examine our expectations with respect to the formation of better soluble complexes we reacted ^{t}bu$_4$-dpttd-H$_2$ with $[RuCl_2(PPh_3)_3]$ according to eqn. (7).

$$[RuCl_2(PPh_3)_3] + {}^t\text{bu}_4\text{-dpttd-H}_2 \xrightarrow[24\ \text{h}]{\text{THF, 20 °C}}$$

$$[Ru(PPh_3)_2({}^t\text{bu}_4\text{-dpttd})] + [Ru(PPh_3)({}^t\text{bu}_4\text{dpttd})] + \text{other products} \quad (7)$$

One obtains a clear green solution from which two compounds could be isolated: the bis-triphenylphosphine complex, in which ^{t}bu$_4$-dpttd^{2-} must act as a tetradentate ligand and the mono-triphenylphosphine complex, which was obtained in single crystals allowing an X-ray structure determination.

Reducing the volume of the reaction solution, adding methanol and storing at −30 °C yield a microcrystalline light brown powder. It analyzed for $[Ru(PPh_3)_2({}^t\text{bu}_4\text{-dpttd})]$ and is well soluble in most solvents from benzene to methanol. The KBr IR spectrum shows the characteristic bands of the ^{t}bu$_4$-dpttd^{2-} as well as the PPh_3 ligands, and in the FD mass spectrum the fragment ion $[M\text{-}PPh_3]^+$ can be observed at $m/e = 956$. The ^{1}H NMR spectrum (see Fig. 5a below) showed peaks of aromatic, C_2H_4 bridge, as well as t-butyl protons in the expected regions, the signals, however, being too numerous to assign to a single isomer. The same is valid for the ^{31}P NMR spectrum; it shows two signals (29.8 ppm/24.9 ppm ref. to H_3PO_4) of unequal intensity indicating at least two diastereomers. These could be the two isomers with *trans* and *cis* thiolato S atoms respectively, which are shown in Fig. 4; regarding the large number of chiral centers in these compounds additional diastereomers have to be considered.

The second product of reaction (7) $[Ru(PPh_3)(^t\text{bu}_4\text{-dpttd})]$ was obtained as orange crystals, when the mother liquor was slowly evaporated at 20 °C. The ^{31}P NMR spectrum of this compound shows one

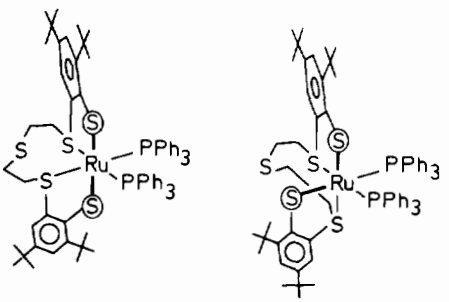

Fig. 4. Isomers of $[Ru(PPh_3)_2(^t\text{bu}_4\text{-dpttd})$ with *trans* and *cis* thiolate S atoms.

TABLE II. Atomic Coordinates of [Ru(PPh_3)(^{t}bu$_4$-dpttd)] (non-H atoms)

Atom	x	y	z	U_{eq}
Ru	0.55820(4)	−0.06671(3)	0.27606(1)	0.0323(2)
S1	0.40445(14)	0.07647(12)	0.21491(5)	0.0447(6)
S2	0.70337(19)	0.01838(16)	0.23347(6)	0.0424(7)
S3	0.62079(17)	0.20887(12)	0.25387(5)	0.0532(6)
S4	0.71658(19)	0.06960(15)	0.33690(6)	0.0390(7)
S5	0.43117(19)	0.14395(14)	0.31734(6)	0.0419(7)
P1	0.48574(15)	−0.07373(11)	0.29387(5)	0.0368(5)
C1	0.4938(8)	0.0548(6)	0.1735(2)	0.0414(28)
C2	0.4355(8)	0.0568(6)	0.1303(2)	0.0521(32)
C3	0.2974(11)	0.0895(11)	0.1166(3)	0.1078(60)
C4	0.2839(15)	0.1896(11)	0.1301(4)	0.1643(101)
C5	0.2625(10)	0.0867(9)	0.0686(2)	0.1656(69)
C6	0.2007(10)	0.0325(11)	0.1332(3)	0.1886(94)
C7	0.5098(8)	0.0268(5)	0.1007(2)	0.0595(28)
C8	0.6382(7)	−0.0032(4)	0.1095(2)	0.0496(25)
C9	0.7068(8)	−0.0369(6)	0.0749(2)	0.0646(31)
C10	0.7230(14)	0.0339(7)	0.0449(3)	0.1723(80)
C11	0.6343(13)	−0.1083(8)	0.0504(4)	0.1446(65)
C12	0.8322(12)	−0.0703(13)	0.0895(3)	0.3152(149)
C13	0.6921(6)	−0.0021(4)	0.1503(2)	0.0441(23)
C14	0.6197(6)	0.0274(4)	0.1813(2)	0.0416(22)
C15	0.8205(6)	0.1127(5)	0.2338(2)	0.0615(28)
C16	0.7930(7)	0.1934(6)	0.2589(3)	0.0681(31)
C17	0.5938(8)	0.2796(5)	0.2969(2)	0.0654(30)
C18	0.4574(7)	0.2611(5)	0.3045(2)	0.0628(28)
C19	0.5144(6)	0.1438(4)	0.3696(2)	0.0423(22)
C20	0.4453(6)	0.1742(5)	0.4001(2)	0.0567(27)
C21	0.4991(7)	0.1776(5)	0.4412(2)	0.0619(28)
C22	0.4263(9)	0.2084(6)	0.4760(2)	0.0865(37)
C23	0.2942(11)	0.2299(16)	0.4630(5)	0.3742(199)
C24	0.4863(12)	0.2835(8)	0.4977(4)	0.1859(78)
C25	0.4180(20)	0.1397(12)	0.5047(5)	0.3556(197)
C26	0.6251(7)	0.1488(5)	0.4495(2)	0.0584(26)
C27	0.7009(7)	0.1182(4)	0.4201(2)	0.0483(24)
C28	0.8406(7)	0.0882(5)	0.4347(2)	0.0583(27)
C29	0.9365(7)	0.1386(5)	0.4106(2)	0.0747(32)
C30	0.8836(9)	0.1070(7)	0.4806(2)	0.0946(40)
C31	0.8515(8)	−0.0151(5)	0.4280(2)	0.0738(32)
C32	0.6410(6)	0.1133(4)	0.3778(2)	0.0368(20)
C33	0.4413(6)	−0.1618(5)	0.2542(2)	0.0450(22)
C34	0.4617(6)	−0.1500(5)	0.2133(2)	0.0496(25)
C35	0.4339(6)	−0.2201(5)	0.1848(2)	0.0570(27)
C36	0.3871(6)	−0.2998(5)	0.1966(2)	0.0604(29)
C37	0.3665(6)	−0.3115(5)	0.2373(2)	0.0585(28)
C38	0.3916(6)	−0.2437(4)	0.2657(2)	0.0463(23)
C39	0.5966(6)	−0.1423(4)	0.3304(2)	0.0416(22)
C40	0.7220(6)	−0.1471(4)	0.3229(2)	0.0468(23)
C41	0.8115(7)	−0.2038(5)	0.3456(2)	0.0606(28)
C42	0.7722(8)	−0.2572(5)	0.3768(2)	0.0688(31)
C43	0.6463(9)	−0.2516(6)	0.3844(2)	0.0768(34)
C44	0.5594(7)	−0.1964(5)	0.3614(2)	0.0591(27)
C45	0.3359(6)	−0.0652(4)	0.3172(3)	0.0493(25)
C46	0.2197(7)	−0.0715(5)	0.2913(3)	0.0655(31)
C47	0.1053(8)	−0.0627(6)	0.3068(4)	0.0922(44)
C48	0.1056(11)	−0.0422(7)	0.3475(4)	0.1073(55)
C49	0.2171(11)	−0.0338(6)	0.3737(3)	0.0951(45)
C50	0.3361(8)	−0.0439(4)	0.3583(2)	0.0658(30)

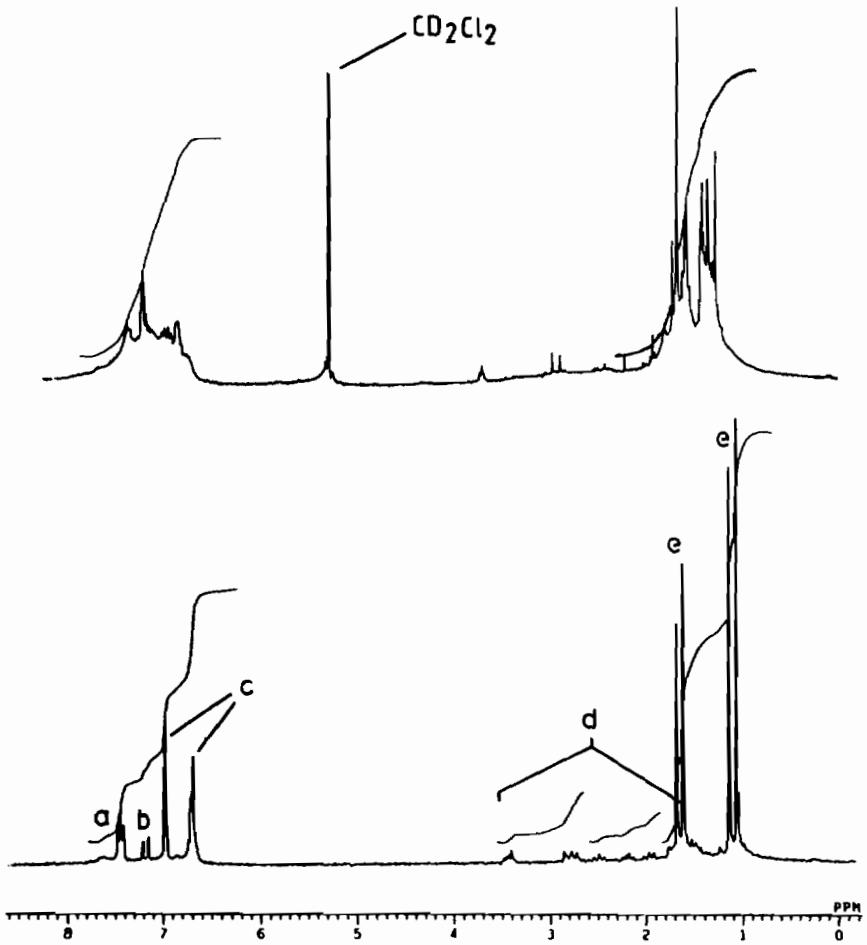

Fig. 5. ^1H NMR spectra of (a) $[Ru(PPh_3)_2(^tbu_4\text{-dpttd})]$ in CD_2Cl_2; (b) $[Ru(PPh_3)(^tbu_4\text{-dpttd})]$ in C_6D_6 (a = C_6D_6, b = aromatic protons of $^tbu_4\text{-dpttd}^{2-}$, c = PPh_3 groups, d = $C_2H_4\text{-S-}C_2H_4$ bridge protons and e = t-butyl protons.

singlet only excluding the presence of diastereomers; in the ^1H NMR spectrum (see Fig. 5b) four t-butyl singlets are observed which show no coalescence up to 100 °C. This indicates that the molecule is rigid and cannot contain a plane or axis of symmetry, as was confirmed by the X-ray structure analysis.

X-ray Structure Analysis of [Ru(PPh$_3$)(^{t}bu$_4$-dpttd)]

Figure 6 shows a view of the molecule and the respective atom numbering. In Table II the atomic coordinates are listed; Table III contains the relevant bond distances and angles.

The ruthenium center is coordinated pseudo-octahedrally by one phosphorus and five sulfur atoms; the thiolato S atoms occupy *trans* positions. Until now it is open to question whether thermodynamic or kinetic reasons determine *trans* or *cis* coordination, respectively, of the thiolato functions in these ligands. In this case the *trans* coordination could be due to repulsion of the t-butyl groups; however, in other $^tbu_4$-dpttd complexes as for example $[Fe(CO)(^tbu_4\text{-dpttd})]$ [16], the ^1H NMR spectra indicate a *cis* coordination of the thiolato S atoms and steric repulsion seems to play no role.

Bond distances as well as angles lie in the same range as observed for other [Ru(thioether-thiolato)] complexes. The Ru–S(thioether) distances (2.320, 2.357 and 2.308 Å) are shorter than the Ru–S(thiolato) distances (2.394 and 2.377 Å); this may be explained by the larger covalent radius of thiolato sulfur as compared to thioether sulfur. Analogous effects have been observed for example in $[\mu\text{-}N_2H_2\{Ru(PPh_3)(dttd)\}_2]$ [17] (Ru–S thioether), 2.282 Å; Ru–S(thiolato), 2.374 Å). Likewise, the Ru–P distances in $[Ru(PPh_3)(^tbu_4\text{-dpttd})]$ and the diazene complex are equal (2.324 and 2.318 Å, respectively).

The X-ray structure analysis shows unambiguously the anticipated position of the t-butyl substituents in isomer c of Fig. 2. Furthermore, it explains plausibly the magnetic nonequivalence of the t-butyl groups. The $S(C_2H_4)_2$ bridge between the two dithiolato ligands spans the $[RuS_1S_2S_4S_5]$ plane in such a way

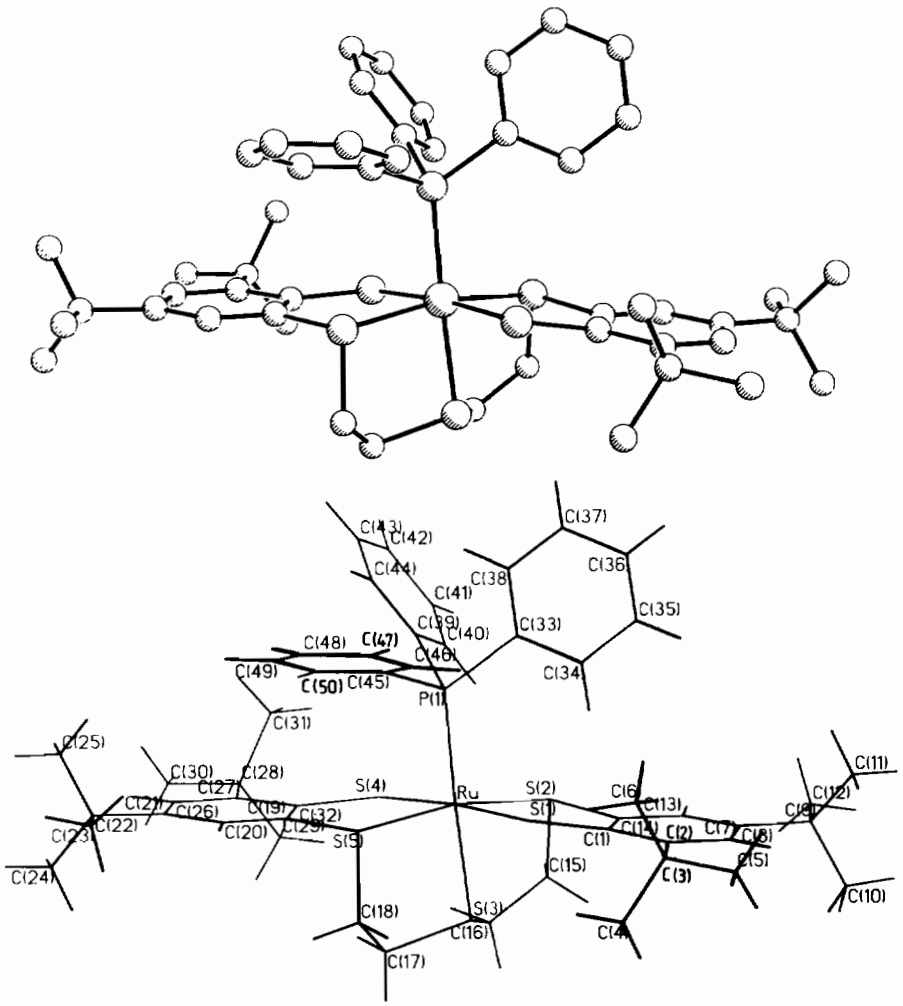

Fig. 6. View of [Ru(PPh$_3$)(^{t}bu$_4$-dpttd)] with the corresponding atom numbering.

that the C_2H_4 groups are placed asymmetrically on one side of the plane formed by ruthenium and the three thioether S atoms S_2, S_3 and S_5 (Fig. 7). This confirmation is rigid up to 100 °C as follows from the ^{1}H NMR spectra.

As mentioned above we wanted to achieve a steric shielding of the thiolato S as well as metal centers by introducing t-butyl groups into the dpttd ligand. The space filling diagram of Fig. 8 shows that this aim is achieved, but apparently not to such an extent, that the steric accessibility of the respective atoms is blocked completely. Hence the good solubility of all [M(^{t}bu$_4$-dpttd)] complexes hitherto investigated might be due not only to the hindrance of thiolate bridging but to other effects as well, for example solvation and lattice energies.

Table IV lists selected spectroscopic data of the synthesized compounds.

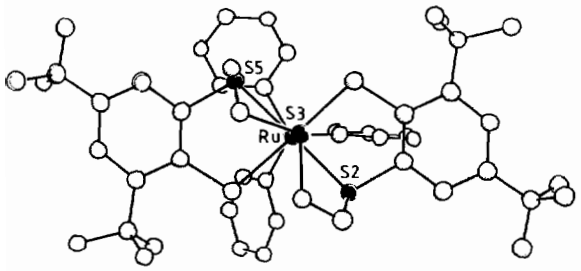

Fig. 7. View of [Ru(PPh$_3$)(^{t}bu$_4$-dpttd)] down the SRuP axis (H atoms omitted).

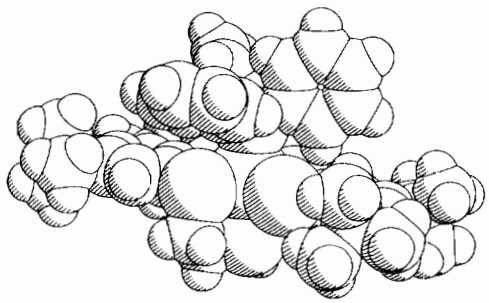

Fig. 8. Space filling diagram of [Ru(PPh$_3$)(^{t}bu$_4$-dpttd)]

TABLE III. Relevant Bond Distances and Angles*

Bond distances (Å)					
Ru–S1	2.377(1)	Ru–S2	2.308(2)	Ru–S3	2.357(2)
Ru–S4	2.394(2)	Ru–S5	2.320(2)	Ru–P1	2.324(2)
S2–C15	1.865(8)	C15–C16	1.501(11)	C16–S3	1.806(7)
S3–C17	1.799(8)	C17–C18	1.510(11)	C18–S5	1.823(7)
S2–C14	1.797(6)	S1–C1	1.771(9)	S4–C32	1.760(6)
S5–C19	1.792(6)	P1–C33	1.850(6)	P1–C39	1.847(6)
P1–C45	1.840(7)				
Bond Angles (°)					
Ru–S2–C14	105.2(2)	Ru–S1–C1	104.5(3)	Ru–S4–C32	107.0(2)
Ru–S5–C19	107.5(2)	Ru–S3–C17	102.0(3)	Ru–S3–C16	100.1(3)
P1–Ru–S3	176.0(1)	P1–Ru–S4	91.5(1)	P1–Ru–S5	93.9(1)
P1–Ru–S2	97.7(1)	P1–Ru–S1	93.1(1)	S2–C15–C16	115.4(5)
C15–C16–S3	108.6(5)	Ru–S5–C18	103.0(3)	S5–C18–C17	112.8(5)
C18–C17–S3	105.9(5)	Ru–P1–C33	121.6(2)	Ru–P1–C39	117.2(2)
Ru–P1–C45	111.6(2)	S4–Ru–S2	93.3(1)	S5–Ru–S1	94.1(1)
S4–Ru–S1	175.3(1)	S5–Ru–S2	168.2(1)	S4–Ru–S3	92.5(1)
S2–Ru–S3	82.1(1)	S5–Ru–S3	86.4(1)	S1–Ru–S1	82.9(1)

[a]See also 'Supplementary Material'.

TABLE IV. Selected Spectroscopic Data of the Compounds

Compound	^{1}H NMR (ppm)[g]		^{31}P NMR (ppm)[h]	KBr IR (cm^{-1})	Mass spectra (m/e)[i]
[Ru(CO)(dpttd)][a,b]	7.80–6.60	(m, C_6H_4, 8)		ν(CO) = 1960	$[M]^+$ = 498
	4.00–3.05	(m, C_2H_4, 8)			
[Ru(PPh_3)$_2$(^{t}bu$_4$-dpttd)][c,d]	6.50–8.40	(m, C_6H_2, C_6H_5, 34)	29.5 25.0		$[M\text{-}PPh_3]^+$ = 956
	3.80–2.60	(m, C_2H_4, 8)			
	2.40–1.00	(m, C_4H_9, 36)			
[Ru(PPh_3)(^{t}bu$_4$-dpttd)][c,e]	7.10	(m, C_6H_2, 4)	41.5		$[M]^+$ = 956
	6.95				
	6.70	(m, C_6H_5, 15)			
	3.50–1.90	(m, C_2H_4, 8)			
	1.10 1.20 1.60 1.70	(s, C_4H_9, 36)			
^{t}bu$_4$-dpttd-H_2[a,f]	7.35–7.10	(m, C_6H_2, 4)		ν(SH) = 2480	$[M]^+$ = 595
	5.80	(s, SH, 2)			
	3.10–2.30	(m, C_2H_4, 8)			
	1.50 1.30	(s, C_4H_9, 36)			

Abbreviations in parenthesis: m = multiplet, s = singlet, relative intensity. [a]60 MHz. [b]In d_7-DMF. [c]270 MHz. [d]In CD_2Cl_2. [e]In C_6D_6. [f]In CCl_4. [g]Ref. to TMS. [h]Ref. to H_3PO_4. [i]Field desorption.

Supplementary Material

Further details of the X-ray crystal structure analysis have been deposited and can be obtained from the Fachinformationszentrum Energie, Physik, Mathematik, D-7514 Eggenstein-Leopoldshafen 2 by citing the deposition No. CSD 52186, the authors and the reference.

Acknowledgements

These investigations were supported by the Deutsche Forschungsgemeinschaft, by the Fonds der Chemischen Industrie, by the Dr. Otto Röhm Gedächtnisstiftung and by a donation of $RuCl_3 \cdot xH_2O$ of the Degussa AG, Hanau. We gratefully acknowledge this support.

References

1 D. Sellmann and G. Binker, *Z. Naturforsch., Teil B, 42,* 341 (1987).

2 (a) R. W. F. Hardy, F. Bottomley and R. C. Burns (eds.), 'A Treatise on Dinitrogen Fixation', Wiley, New York, 1979; (b) A. Müller and B. Krebs (eds.), 'Sulfur, Its Significance for Chemistry, for the Geo-, Bio- and Cosmosphere and Technology', Studies in Inorganic Chemistry', Vol. 5, Elsevier Science Publishers, Amsterdam, 1984; (c) S. D. Conradson, B. K. Burgess, W. E. Newton, K. O. Hodgson, J. W. McDonald, J. F. Rubinson, S. F. Gheller, L. E. Mortenson, M. W. W. Adams, P. K. Mascharak, W. A. Armstrong and R. H. Holm, *J. Am. Chem. Soc., 107,* 7935 (1985).

3 D. Sellmann and W. Reisser, *Z. Naturforsch., Teil B, 39,* 1268 (1984); D. Sellmann and L. Zapf, *Z. Naturforsch., Teil B, 40,* 368 (1985).

4 D. Sellmann and E. Unger, *Z. Natuforsch., Teil B, 34,* 1096 (1979).

5 D. Sellmann and U. Kleine-Kleffmann, *J. Organomet. Chem., 247,* 307 (1983).

6 J. Degani and R. Fochi, *Synthesis, 7,* 471 (1976).

7 W. Steinkopf, J. Herold and J. Stöhr, *Ber. Deutsch. Chem. Ges., 53,* 1007 (1920).

8 D. Sellmann, G. Freyberger, E. Böhlen, R. Eberlein, G. Huttner and L. Zsolnai, *J. Organomet. Chem.,* in press.

9 (a) M. I. Bruce and F. G. A. Stone, *J. Chem. Soc. A,* 1238 (1967); (b) D. Sellmann and E. Böhlen, *Z. Naturforsch., Teil B, 37,* 1026 (1982).

10 T. A. Stephenson and G. Wilkinson, *J. Inorg. Nucl. Chem., 28,* 945 (1966).

11 J. Chatt, G. J. Leigh and A. P. Storace, *J. Chem. Soc. A,* 1380 (1971).

12 J. M. Fletcher, J. L. Jenkins, F. M. Lever, F. S. Martin, A. R. Powell and R. Todd, *J. Inorg. Nucl. Chem., 1,* 378 (1955).

13 J. P. Evans, A. Spencer and G. Wilkinson, *J. Chem. Soc., Dalton Trans.,* 204 (1973).

14 G. M. Sheldrick, 'SHELXTL', Programmsystem, Göttingen, 1984.

15 H. Günther, 'NMR-Spektroskopie', 1. Aufl., Thieme Verlag, Stuttgart, 1973.

16 D. Sellmann and G. Binker, *J. Organomet. Chem.,* in press.

17 D. Sellmann, E. Böhlen, M. Waeber, G. Huttner and L. Zsolnai, *Angew. Chem., 97,* 984 (1985); *Angew. Chem., Int. Ed. Engl., 24,* 981 (1985).